TRANSITIONAL AND PRE-TRANSITIONAL DISKS: GAP OPENING BY MULTIPLE PLANETS?

Zhaohuan Zhu[1], Richard P. Nelson[2], Lee Hartmann[1], Catherine Espaillat[3,4], and Nuria Calvet[1]
[1] Department of Astronomy, University of Michigan, 500 Church Street, Ann Arbor, MI 48109, USA; zhuzh@umich.edu, lhartm@umich.edu, ncalvet@umich.edu
[2] Astronomy Unit, Queen Mary, University of London, Mile End Road, London E1 4NS, UK; r.p.nelson@qmul.ac.uk
[3] Center for Astrophysics, 60 Garden Street, Cambridge, MA 02138, USA; cespaillat@cfa.harvard.edu

ABSTRACT

We use two-dimensional hydrodynamic simulations of viscous disks to examine whether dynamically interacting multiple giant planets can explain the large gaps (spanning over one order of magnitude in radius) inferred for the transitional and pre-transitional disks around T Tauri stars. In the absence of inner disk dust depletion, we find that it requires three to four giant planets to open up large enough gaps to be consistent with inferences from spectral energy distributions, because the gap width is limited by the tendency of the planets to be driven together into 2:1 resonances. With very strong tidal torques and/or rapid planetary accretion, fewer planets can also generate a large cavity interior to the locally formed gap(s) by preventing outer disk material from moving in. In these cases, however, the reduction of surface density produces a corresponding reduction in the inner disk accretion rate onto the star; this makes it difficult to explain the observed accretion rates of the pre-transitional/transitional disks. We find that even with four planets in disks, additional substantial dust depletion is required to explain observed disk gaps/holes. Substantial dust settling and growth, with consequent significant reductions in optical depths, is inferred for typical T Tauri disks in any case, and an earlier history of dust growth is consistent with the hypothesis that pre-transitional/transitional disks are explained by the presence of giant planets. We conclude that the depths and widths of gaps and disk accretion rates in pre-transitional/transitional disks cannot be reproduced by a planet-induced gap opening scenario alone. Significant dust depletion is also required within the gaps/holes. Order-of-magnitude estimates suggest that the mass of small dust particles ($\lesssim 1\,\mu$m) relative to the gas must be depleted to 10^{-5} to 10^{-2} of the interstellar medium value, implying a very efficient mechanism of small dust removal or dust growth.

Key words: accretion, accretion disks – stars: formation – stars: pre-main sequence

Online-only material: color figures

1. INTRODUCTION

The transitional and pre-transitional disks around young stars exhibit strong dust emission at wavelengths $\gtrsim 10\,\mu$m, while showing significantly reduced fluxes relative to typical T Tauri disks at shorter wavelengths (e.g., Calvet et al. 2002, Calvet et al. 2005; D'Alessio et al. 2005; Espaillat et al. 2007, 2008). In the pre-transitional disks, there is evidence for emission from warm, optically thick dust near the star (Espaillat et al. 2007, 2008, 2010), while in the transitional disks the emission at $\lesssim 10\,\mu$m appears to be due entirely to optically thin dust (Calvet et al. 2002, 2005; Espaillat et al. 2010). The depletion of near- to mid-infrared emission is generally interpreted as being due to evacuation of the disk interior to scales $\sim$5–50 AU (Marsh & Mahoney 1992; Calvet et al. 2002, 2005; Rice et al. 2003; Schneider et al. 2003; Espaillat et al. 2007, 2008, 2010; Hughes et al. 2009), an interpretation confirmed in some cases via direct submillimeter imaging (e.g., Piétu et al. 2006; Brown et al. 2007, 2009; Hughes et al. 2009; Andrews et al. 2009).

One proposed mechanism for clearing inner disks while leaving the outer disk relatively undisturbed is the formation of giant planets, which can open gaps in disks (e.g., Lin & Papaloizou 1986; Marsh & Mahoney 1992; Nelson et al. 2000; Calvet et al. 2002; Rice et al. 2003), and which are expected to form initially at relatively small disk radii due to the shorter evolutionary timescales compared with the outermost disk. However, there are three observational challenges, as discussed

further in Section 2, which theoretical explanations of these systems must confront.

First, the transitional and pre-transitional disk systems exhibit average gas accretion rates close to T Tauri disk accretion rates ($\sim 10^{-8}\,M_{\odot}$ yr^{-1}; Hartmann et al. 1998) onto their central stars (e.g., Calvet et al. 2002, 2005; Espaillat et al. 2007, 2008; Najita et al. 2007). Maintaining this accretion requires either a significant mass reservoir interior to the disk-clearing planets or some way of allowing mass from the outer disk to move past the gap-clearing planets.

Second, the cleared regions in these disks are large (e.g., Espaillat et al. 2010). In the case of the transitional disks, the optically thin region must extend from radii as large as tens of AU all the way in to the central star. Even the pre-transitional disks, which have evidence for optically thick dust emission in the innermost regions, must have large disk gaps. Furthermore, the spectral energy distribution (SED) modeling suggests that the detected optically thick region may only extend to radii $\sim$1 AU, with an extremely dust-free region beyond, until reaching the outer optically thick disk (Espaillat et al. 2010; Section 2).

Third, the requirement that the gap/hole be optically thin implies that the mass of dust in sizes of order a micron or less must be extremely small. Thus, either the planet-induced gap is very deep and effectively cleared of gas and dust or the dust abundance is reduced by many orders of magnitude from abundances in the diffuse interstellar medium (ISM).

These three conditions must be fulfilled simultaneously. Photoevaporation has been proposed as one gap/hole clearing

---

[4] NSF Astronomy, and Astrophysics Postdoctoral Fellow.

mechanism (Alexander & Armitage 2007, 2009), but requires the mass loss rate by the photoevaporation to be comparable to the disk accretion rate. Initial estimates of photoevaporative mass loss suggested values of $\sim 4 \times 10^{-10}\,M_\odot$ yr^{-1} (Clarke et al. 2001), which would not be rapid enough to counteract accretion. More recent estimates suggest higher values, perhaps as much as $\sim 10^{-8}\,M_\odot$ yr^{-1} due to the inclusion of X-rays (Gorti & Hollenbach 2009; Owen et al. 2010); however, the highest values are problematic, because then it becomes difficult to understand why so many T Tauri disks last for several Myr with accretion rates smaller than $10^{-8}\,M_\odot$ yr^{-1} (Hartmann et al. 1998).

Najita et al. (2007) suggested that giant planets might explain the transitional disks by creating a gap while still maintaining accretion onto the central star. Najita et al. argued that there is some evidence of reduction in the accretion rates in transitional disks relative to the so-called primordial disks, perhaps by an order of magnitude, and that this was consistent with simulations of a single giant planet in the studies by Lubow & D'Angelo (2006) and Varnière et al. (2006). However, as discussed in Section 2, the accretion rates of the pre-transitional/transitional disks are not very low in absolute magnitude. Moreover, while Varnière et al. (2006) were able to produce a large cleared inner region with a single planet, the study of Crida & Morbidelli (2007) calls this result into question (see also Section 3).

In this paper, we consider whether disk gap formation by a multiple planet system can satisfy the following requirements: (1) creation of a gap extending over a large range in radius, (2) maintenance of the inner disk accretion rate by flow through the planet-created gap, and (3) sufficient reduction in the disk surface density within the gap such that extreme depletion of disk dust is not essential. We examine the problem in the context of viscous disks, with improvements over some previous simulations, including a more realistic temperature distribution and an improved inner boundary condition. We find that while multiple giant planets can indeed open large gaps, it is difficult to explain the inferred properties of the pre-transitional/transitional disks without invoking substantial depletion of small dust. We offer a speculative scenario in which combined dust depletion and planet formation explains the observations.

2. INFERRED PROPERTIES OF PRE-TRANSITIONAL/TRANSITIONAL DISKS

We first present a summary of properties of some of the known pre-transitional/transitional systems in Table 1 as derived from analysis of optical, infrared, and millimeter SEDs, including the pre-transitional disk systems LkCa 15, UX Tau A, Rox 44, and of the transitional disk GM Aur. The parameters are mostly taken from Espaillat et al. (2010), where the methods used to derive these estimates are discussed.

As indicated in Table 1, the estimated maximum extent of the inner optically thick region in the pre-transitional disks is ~ 0.2–0.4 AU, while the inner edges of the optically thick outer disks lie at ~ 40–70 AU. The location of the inner edge of the outer disk inferred from SED modeling is consistent with that derived using millimeter interferometry (Piétu et al. 2006; Andrews et al. 2009; S. Andrews 2010, private communication). The maximum extent of the inner disk is less certain and is based on SED modeling of the near-infrared emission. In this wavelength region, the flux in pre-transitional disks is dominated by the emission of the inner wall. To limit the size of the optically thick disk behind the inner wall, Espaillat et al. (2010) varied the maximum extent of this inner disk and fitted it to the SED of the

Table 1
Stellar and Model Properties of LkCa 15, UX Tau A, Rox 44, and GM Aur from Espaillat et al. (2010)

Properties	LkCa 15	UX Tau A	Rox 44	GM Aur
	Stellar Properties			
M_* ($M_\odot$)	1.3	1.5	1.3	1.1
T_* (K)	4730	5520	4730	4350
$\dot{M}$ ($M_\odot$ yr^{-1})	3.3×10^{-9}	1.1×10^{-8}	9.3×10^{-9}	7.2×10^{-9}
	Optically Thick Inner Wall			
$R^i_{\rm wall}$ (AU)	0.15	0.15	0.25	. . .
	Optically Thick Inner Disk			
$R_{\rm inner\,disk}$ (AU)	<0.19	<0.21	<0.4	. . .
$M_{\rm inner\,disk}$ ($M_\odot$)	$<2 \times 10^{-4}$	$<6 \times 10^{-5}$	$<8 \times 10^{-5}$	. . .
	Optically Thick Outer Wall			
$R^o_{\rm wall}$ (AU)	58	71	36	20
	Optically Thick Outer Disk			
ϵ	0.001	0.001	0.01	0.5
α	0.0005	0.004	0.006	0.002
$M_{\rm disk}$ ($M_\odot$)	0.1	0.04	0.03	0.16
	Optically Thin Dust in Gap/Hole			
M ($M_\odot$)	2×10^{-11}	. . .	2×10^{-11}	2×10^{-12}
$a_{\rm min}$ (μm)	0.005	. . .	0.005	0.005
$a_{\rm max}$ (μm)	0.25	. . .	0.25	0.25
$R_{\rm out,thin}$ (AU)	4	. . .	2	1

object. The value listed in Table 1 represents the largest $R_{\rm inner\,disk}$ that does not produce too much excess emission, assuming a typical disk flaring structure. A caveat is that if the inner wall is "puffed up" relative to the disk behind it (e.g., Natta et al. 2001), or if the dust behind the inner wall is more settled than the wall, the inner disk would be in shadow and not emit strongly. However, we note that the near-infrared interferometric observations by Pott et al. (2010) are consistent with the dust emission being confined to a small radius as inferred from the SED modeling. The amount of emitting optically thin sub-micron-sized dust is small, $\sim 10^{-11}\,M_\odot$.

Transitional disks do not have the inner optically thick disk observed in the pre-transitional disks. The transitional disk of GM Aur has a 20 AU hole, based on modeling both the SED and submillimeter interferometric visibilities (Hughes et al. 2009). About $10^{-12}\,M_\odot$ of sub-micron-sized optically thin dust is necessary within the inner AU of the hole to reproduce the observed silicate emission in the near-infrared. Calvet et al. (2005) inferred that the inner emitting, optically thin dust in GM Aur is confined to within 5 AU by modeling its SED. While SED modeling is nonunique, the interferometric observations of Pott et al. (2010) indicated that this dust is confined within even smaller radii, $\lesssim 0.15$ AU (see also Akeson et al. 2005). Thus, as stated by Pott et al. (2010), the pre-transitional/transitional disks are often characterized by distinct dust zones "which are not smoothly connected by a continuous distribution of optically thick material," which may be interpreted as the result of a highly cleared gap with an inner region of optically thin or thick dust.

The final important point to be made is that, as shown in Table 1, the gas accretion rates onto the central stars are substantial, ~ 0.3–$1 \times 10^{-8}\,M_\odot$ yr^{-1}, not much lower than rates typical of T Tauri stars (e.g., Hartmann et al. 1998). These high gas accretion rates agree with significant gas emission detected at the inner disk by *Spitzer* (Najita et al. 2010). Thus, the depletion of dust optical depth appears to be orders of magnitude larger than any reduction in the gas accretion rate. This poses

strong constraints on theories of the origin of pre-transitional/
transitional disk structure, as we now show.

3. METHODS: DISK–PLANET SIMULATIONS

To simulate multiple giant planet systems, we use FARGO
(Masset 2000). This is a two-dimensional (2D) hydrodynamic
code which utilizes a fixed grid in cylindrical polar coor-
dinates (R, ϕ). FARGO uses finite differences to approxi-
mate derivatives, and the evolution equations are divided into
source and transport steps, similar to those of ZEUS (Stone &
Norman 1992). However, an orbital advection scheme has been
incorporated which reduces the numerical diffusivity and sig-
nificantly increases the allowable time step as limited by the
Courant–Friedrichs–Lewy (CFL) condition. Thus FARGO en-
ables us to study the interaction between the disk and embedded
planets over a full viscous timescale for disks whose inner radii
are considerably smaller than the radial locations of the embed-
ded planets, which is an essential requirement for studying large
gaps created by multiple planet systems.

We assume a central star mass of $1\,M_\odot$ and a fully viscous
disk. We further assume a radial temperature distribution $T =
221(R/\mathrm{AU})^{-1/2}$ K, which is roughly consistent with typical T
Tauri disks in which irradiation from the central star dominates
the disk temperature distribution (e.g., D'Alessio et al. 2001).
The disk is locally isothermal. The adopted radial temperature
distribution corresponds to an implicit ratio of disk scale height
to cylindrical radius $H/R = 0.029(R/\mathrm{AU})^{0.25}$. This differs
from the $H/R = $ constant assumption used in many previous
simulations, which implies a temperature distribution $T \propto R^{-1}$,
which is inconsistent with observations. Consequently, our
assumed temperature distribution with a constant viscosity
parameter α ($\nu = \alpha c_s^2/\Omega$, where ν is the kinematic viscosity,
c_s is the sound speed, Ω is the angular velocity) leads to a
steady-disk surface density distribution $\Sigma \propto R^{-1}$ instead of
the $\Sigma \propto R^{-1/2}$ that would result from assuming either that
both H/R and $\dot{M}$ are constant or both ν and viscous torque
$(-2\pi R\Sigma\nu R^2 d\Omega/dR)$ are constant. This makes a significant
difference in the innermost disk surface densities, and thus the
implied inner disk optical depths in our models will be larger.

We set $\alpha = 0.01$ for the standard cases. Given our assumed
disk temperature distribution, we set the initial disk surface
density to be $\Sigma = 178\,(R/\mathrm{AU})^{-1}\,(0.01/\alpha)$ g cm^{-2} from
$R \sim 1$–200 AU, which yields a steady disk solution with an
accretion rate $\dot{M} \sim 10^{-8}\,M_\odot$ yr^{-1}, typical of T Tauri disks
(Gullbring et al. 1998; Hartmann et al. 1998). The mass within
the radius R_{out} is then

$$M(R < R_{\mathrm{out}}) = \int_{R_{\mathrm{in}}}^{R_{\mathrm{out}}} 2\pi R\Sigma(R)dR$$
$$= 1.26 \times 10^{-4}\frac{0.01}{\alpha}\left(\frac{R_{\mathrm{out}}}{\mathrm{AU}} - \frac{R_{\mathrm{in}}}{\mathrm{AU}}\right)M_\odot. \quad (1)$$

With $R_{\mathrm{in}} = 1$ AU, $R_{\mathrm{out}} = 200$ AU, and $\alpha = 0.01$, the total disk
mass is thus $0.025\,M_\odot$, reasonably consistent with observational
estimates (e.g., Andrews & Williams 2005).

We use logarithmic spacing for the radial grid to span the
large dynamic range needed. The azimuthal resolution is 256
cells covering 2π radians, and the radial resolution is adjusted
so that each grid cell is square ($R\Delta\theta = \Delta R$).

Each planet in the disk can interact gravitationally with the
other planets and with the disk. The interactions among multiple
planets and the star are solved using a fifth-order Runge–Kutta

integrator. Each planet feels the acceleration from the disk given
by

$$\mathbf{a} = -G \int_S \frac{\Sigma(\mathbf{r}')(\mathbf{r}_p - \mathbf{r})'dS}{(|\mathbf{r}' - \mathbf{r}_p|^2 + \epsilon^2)^{3/2}}, \quad (2)$$

where the integral is performed over the whole disk area S. Here,
$\mathbf{r}_p$ denotes the planet's position and ϵ is the smoothing length
set to be $0.6H$, where H is the disk scale height at the planet's
orbit.

To accurately simulate close encounters between planets, an
additional time step constraint is applied. For each pair of planets
(i, j), we calculate the minimum time step,

$$dt = \frac{1}{400}\min\left(\frac{2\pi}{\Omega_{\mathrm{ij}}}\right), \quad (3)$$

where $\Omega_{ij} = [G(m_i + m_j)/|\mathbf{r}_i - \mathbf{r}_j|^3]^{1/2}$ is an estimate of
the orbital frequency that each pair of planets (with masses
m_i and m_j) would have if they were in orbit around each
other, with $|\mathbf{r}_i - \mathbf{r}_j|$ being the absolute value of the distance
between them. Throughout most of the simulations the time
step size is determined by the normal CFL condition, but when
a close encounter occurs the interaction is resolved by allowing
Equation (3) to determine the time step size.

Accretion onto the planet is simulated by depleting the
disk surface density within the planet's Hill radius, $R_H =
(M_P/3M_*)^{1/3}r_p$, where M_P and M_* are the planet and stellar
masses, respectively. This approach is required because of the
necessity to evolve the disk–planet system for longer than the
viscous timescale measured at the disk outer edge, which forces
us to adopt a relatively low numerical resolution that prevents us
from modeling accurately the gas flow onto the planet within the
planet Hill sphere. Defining a dimensionless scaling parameter,
f, we deplete the disk within $0.45R_H$ at a rate

$$\frac{d\Sigma}{dt} = -\frac{2\pi}{fT_P}\Sigma, \quad (4)$$

and between 0.45 and $0.75\,R_H$ at a reduced rate

$$\frac{d\Sigma}{dt} = -\frac{2\pi}{3fT_P}\Sigma, \quad (5)$$

where T_P is the orbital period of the planet.[5] We term f the planet
accretion timescale parameter. During the intermediate stages
of giant planet formation, after the formation of the solid core,
but prior to the onset of rapid gas accretion, gas slowly settles
onto the planet at a rate determined by the Kelvin–Helmholtz
timescale. Depending on the opacity of the planet envelope,
this phase lasts for up to a few Myr (Pollack et al. 1996;
Papaloizou & Nelson 2005; Movshovitz et al. 2010). Once
the planet reaches a value of ~ 35–$50\,M_\oplus$, rapid gas accretion
onto the planet is able to ensue, relatively unimpeded by the
thermodynamic evolution of the atmosphere, and the planet can
grow quickly to become a giant. During this final phase of
growth, however, the planet contracts rapidly, becoming much
smaller than its Hill sphere, and further gas accretion must occur
via flow through a circumplanetary disk (Papaloizou & Nelson
2005). Simulations presented by Ayliffe & Bate (2009) suggest
that the circumplanetary disk has a radius $R_{\mathrm{cp}} \simeq R_H/3$ and

---

[5] Note that our parameterization is different from the publicly available
version of FARGO.

aspect ratio $(H/R)_{cp} \simeq 0.5$. Adopting these values, the viscous timescale for the circumplanetary disk is

$$\tau_{acc} \simeq 1/(5\pi\alpha)T_P \equiv f/(2\pi), \tag{6}$$

from which we see that $f = 2/(5\alpha)$. Varying the value of α between representative values of 10^{-2} and 10^{-3}, leads to variations of the accretion time of between ~ 6 and 60 planet orbits. Since f is poorly constrained, we vary it by two orders of magnitude in this work: $1 \leqslant f \leqslant 100$.

Observations of exoplanets allow us to place some constraints on the value of f. Once gap formation ensues, mass accretion into the planet Hill sphere is controlled by the rate at which material is supplied to the planet by viscous evolution of the protoplanetary disk. A mass accretion rate of $10^{-8} M_\odot$ yr^{-1} implies growth of the planet to masses $\geqslant 10 M_J$ over disk lifetimes of a few Myr if $f = 1$. Given that exoplanets with masses $> 10 M_J$ are relatively rare, this suggests that $f = 1$ is a reasonable lower limit. A value of $f = 100$ implies mass accretion onto the planet at the rate $\sim 10^{-9}$ to $10^{-10} M_\odot$ yr^{-1} (10^{-6} to $10^{-7} M_J$ yr^{-1}). Such low values of f can barely explain the numerous exoplanets with masses in the range 1–5 M_J, suggesting that $f = 100$ is a reasonable upper limit.

We initiate most of our simulations with relatively low planet masses (details are given later in this section), and the fact that planets grow slowly if $f = 100$ means that during our simulations rapid type I and type III migration are likely to dominate the evolution of the planet orbits (Masset & Papaloizou 2003). To avoid this, we initiate simulations with $f = 100$ with the smaller value $f = 10$ until a gap opens and the planet reaches 1 M_J, at which point f is switched back to 100. The mass and momentum of the depleted portion of the disk are added to the planet's mass and momentum, such that the planet's migration will be (modestly) affected by its accretion from the disk.

As discussed by Crida et al. (2007), a standard open inner boundary condition (Stone & Norman 1992) in a fixed 2D grid can produce an unphysically rapid depletion of material through the inner boundary in the presence of the planets. There are two reasons for this. First, due to waves excited by the planet, the gas in the disk can have periodic inward and outward radial velocities larger than the net viscous velocity of accreting material. Thus, with the normal open boundary, material can flow inward while there is no compensating outflow allowed. Second, the orbit of the gas at the inner boundary is not circular due to the gravitational potential of the planets; again, as material cannot pass back out through the inner boundary, rapid depletion of the inner disk material is enhanced. As we are interested in the amount of gas depletion in the disk inward of the planet-induced gap(s) over substantial evolutionary timescales, it is important to avoid or minimize this unphysical mass depletion.

Crida et al. (2007) were able to ameliorate this problem by surrounding the 2D grid by extended one-dimensional (1D) grids (see their Figure 5). We follow Pierens & Nelson (2008), who found reasonable agreement with the Crida et al. results while using a 2D grid only by limiting the inflow velocities at the inner boundary to be no more than a factor β larger than the viscous radial velocity in a steady state,

$$v_{rs} = -\frac{3\nu_{in}}{2R_{in}}, \tag{7}$$

where ν_{in} and R_{in} are the viscosity and radius at the inner boundary. Pierens & Nelson (2008) found satisfactory behavior for $\beta = 5$ in their simulations, based on a comparison with

1D–2D calculations. As our parameters differ somewhat from those of Pierens & Nelson, we also made a comparison with the 1D–2D setup in FARGO described by Crida et al. (2007), and found that $\beta = 3$ provided reasonable results. We adopted the normal open boundary condition as our outer boundary condition.[6] The open outer boundary allows mass to leave the computational domain, and in strongly perturbed disks containing massive planets this can cause a noticeable reduction in the disk mass over long timescales which in principle can reduce the gas accretion rate through the disk. But because this effect requires a long time to develop, its effect on our results is very modest.

We do not use the 1D–2D grid method in this paper because in some cases our planet masses grow considerably larger than one Jupiter mass, and the non-circular motion of the gas close to the 2D boundary is significant enough so that an artificial gap is opened at the interface between the 1D and 2D grids, which causes the code to crash.

Since our numerical inner boundary is far away from the real disk inner boundary, we assign the ghost zone density to be

$$\Sigma_g = \Sigma_1 \frac{R_1}{R_g} \tag{8}$$

to simulate the power-law section of the constant α disk similarity solution, where subscript g denotes the ghost zone and 1 the first active zone.

In order to reduce problems related to relaxation from initial conditions, and to mimic the effect of accreting gas onto a protoplanet at the beginning of the rapid gas accretion phased discussed earlier in this section, we performed the following steps. First, we allowed for the planet mass to grow linearly from zero to its initial mass during the first 5000 years. For simulations where the planet accretes gas from the disk the initial mass is $0.1 M_J$, and is 1 M_J otherwise. During this period the planet does not feel the gravitational force from the disk and does not accrete gas. This step is necessary; otherwise the sudden presence of a one Jupiter mass planet in a Keplerian disk disturbs the disk so much that the excited acoustic waves can be present in the disk for a long time,[7] and these waves gradually deplete the disk mass by creating flows through the outer boundary. Then we allow the planet to start accreting at 10^4 yr. Finally, we allow the planet to feel the disk's gravitational force gradually, starting at 10^4 yr and with full force at $t = 2 \times 10^4$ yr. This gradual ramping up of the gravitational effects is also important, since a sudden turn-on of gravity can kick the planet outside the gap it just opened. As well as being convenient from a computational point of view, this approach also ensures that gap formation arises both because of tidal torques and accretion onto the planet.

Problems with boundary conditions also led us to perform simulations without the indirect terms in the gravitational potential experienced by the disk and planets. These terms arise when working in the non-inertial reference frame based on the central star, as they account for the acceleration of the central star by the disk and planets. The resulting non-circular motions can cause problems at both inner and outer boundaries of our circular grid similar to those discussed above. Given the importance of these issues to our investigation of the disk surface density distribution exterior to gaps, we therefore did not include the indirect terms initially. We subsequently recomputed

---

[6] This is different from the publicly available version of FARGO.
[7] Waves can reflect back from the boundary even with the open boundary condition.

Table 2
Models

Case Name	R_{in} (AU)	R_{out} (AU)	$\Sigma_{1\,AU}$ (g cm^{-2})	R_P[a] (AU)	M_P[b] (M_J)	Acc[c] f
PN	1.5	200	178	...	...	...
P1AN	1.5	200	178	20	1	No
P1A100	1.5	200	178	20	0.1	100
P1A10	1.5	200	178	20	0.1	10
P1A1	1.5	200	178	20	0.1	1
P2AN	0.75	200	178	12.5/20	1	No
P2A100	0.75	200	178	12.5/20	0.1	100
P2A10	0.75	200	178	12.5/20	0.1	10
P2A1	0.75	200	178	12.5/20	0.1	1
P3AN	0.5	200	178	7.5/12.5/20	1	No
P3A100	0.5	200	178	7.5/12.5/20	0.1	100
P3A10	0.5	200	178	7.5/12.5/20	0.1	10
P3A1	0.5	200	178	7.5/12.5/20	0.1	1
P4AN	0.5	200	178	5/7.5/12.5/20	1	No
P4A100	0.5	200	178	5/7.5/12.5/20	0.1	100
P4A10	0.5	200	178	5/7.5/12.5/20	0.1	10
P4A1	0.5	200	178	5/7.5/12.5/20	0.1	1

Notes.
[a] The initial planet radii. The radii can change with time due to migration and planet–planet interaction.
[b] The initial planet mass. If Acc is not "No," the mass can increase with time due to accretion from the disk.
[c] The accretion coefficient f is defined in Equations (4) and (5).

the models P4AN and P4A10 (see the following section) to include the indirect terms to ensure that the planetary stability properties and the gap structures that we report in this paper remain effectively unchanged; we do indeed find that this is the case. (The result for the P4A10 case with indirect terms is shown in Figure 8.) In performing these tests with the indirect terms we found it necessary to adopt the wave-damping boundary condition described in De Val-Borro et al. (2006) in order for the disk to remain well behaved at the outside edge. Adopting this boundary condition has very little influence, however, on the structure of the gap or the stability properties of the planetary systems, so we believe that the results presented in this paper provide an accurate description of the features most important for comparing with observed pre-transitional/transitional disk structures.

4. RESULTS

We performed simulations with one, two, three, and four planets in the disk to study planet gap opening and gas flowing through gaps. The disk simulations evolve over 1 million years (Myr), which is the characteristic viscous timescale at $R \sim 100$ AU, and is also shorter than the timescale over which most T Tauri disks are observed to clear. The properties of the simulations are summarized in Table 2.

4.1. Viscous Disks with One Planet

For comparison and test purposes, we first calculated a case without planets (case PN). The disk evolves as expected for a viscous disk with constant α, maintaining a surface density $\Sigma \propto R^{-1}$ and a nearly constant mass accretion rate of $10^{-8}\,M_\odot$ yr^{-1}.

We then placed a single $1M_J$ (ramping up to $1M_J$ during the first 5000 yrs as discussed in Section 3), non-accreting planet in the disk at 20 AU initially (case P1AN). After 0.5 Myr the planet has migrated in to $\sim$8 AU (Figure 1). The azimuthally averaged surface density within the gap is reduced by about an

order of magnitude (solid curve in the left panel of Figure 1). The resulting gap is relatively shallow, as expected due to the high disk viscosity (Lin & Papaloizou 1993; Crida & Morbidelli 2007) and relatively large disk thickness at 20 AU where $H/R \simeq 0.061$. The viscous criterion for gap formation is $q > 40/R_e$, where q is the planet–star mass ratio and R_e is the Reynolds number. At 20 AU in a disk with $\alpha = 0.01$ clear gap formation is only expected for a planet with mass $M_P > 1.5M_J$. The thermal condition for gap formation, which determines if the disk response to the planet is nonlinear, requires $R_H > H$ at the planet location, which is only just satisfied for a $1M_J$ planet at 20 AU.

Because the planet is not allowed to accrete from the disk, and the tidal torques that it exerts are not strong enough to truncate the mass flow through the disk, accretion flow is channeled through the gap and arrives in the inner disk. Due to the continuous replenishment from the outer disk beyond the planet, the inner disk can maintain the $10^{-8}M_\odot$ yr^{-1} accretion rate onto the central star (right panel of Figure 1). As expected, the inner disk surface density is not strongly affected by the presence of the planet and is close to that obtained in the unperturbed viscous disk model PN described above.

We next allowed the planet to accrete, at a rate controlled by the parameter f as described in Section 2. The planet starts out with a mass of $0.1M_J$ and is again placed at 20 AU. If $f = 1$ (case P1A1), after the initial phase when the planet accretes material around it and opens a gap, the inner disk surface density decreases by one order of magnitude, and consequently the accretion rate onto the central star also decreases by one order of magnitude ($10^{-9}M_\odot$ yr^{-1}) relative to the non-accreting case. This case is nearly equivalent to that studied by Lubow & D'Angelo (2006),[8] who similarly found that $\sim$90% of the disk accretion flows onto the planet, leaving only $\sim$10% to pass through into the inner disk. On the other hand, we have much higher disk surface densities inside the gap than do Varnière et al. (2006). As discussed in Section 2, this difference is almost certainly due to the difference in the inner boundary condition. In test calculations performed which did not use the β-limiter on the radial velocity (Section 2), we observed a similar rapid depletion of the inner disk (see also Crida & Morbidelli 2007).

As the planet mass grows with time, the gap becomes wider and deeper due to the removal of gas from the disk and the increasing effectiveness of the tidal torques. As 90% of the accreting disk mass is added to the planet at a rate $\sim 10^{-8}M_\odot$ yr^{-1}, the planet grows to $10\,M_J$ after 1 Myr (left panel in Figure 2), so that the gap is much deeper than the case where the planet does not accrete (left panel in Figure 1).

If $f = 10$ (case P1A10), the inner disk surface density and mass accretion rate onto the central star is reduced to 30% of the non-accreting planet case. Because the planet accretes more slowly than in the $f = 1$ case, the planet is less massive (right panel in Figure 2) and so the gap is shallower. The eccentricity for this case is lower than for the P1A1 case (this is also true for multiple planet cases, as discussed below).

If $f = 100$ (case P1A100), the inner disk surface density and accretion rate onto the central star is barely affected by the planet (dotted curve in Figure 1). Only 10% of the mass flowing through the gap accretes onto the planet. Thus, it takes 1 Myr for the planet to grow to $1M_J$. The accretion rates show an initial rapid decay due to the inner disk adjusting to the reduced flow from the outer disk; thereafter, the accretion rates show a slow

---

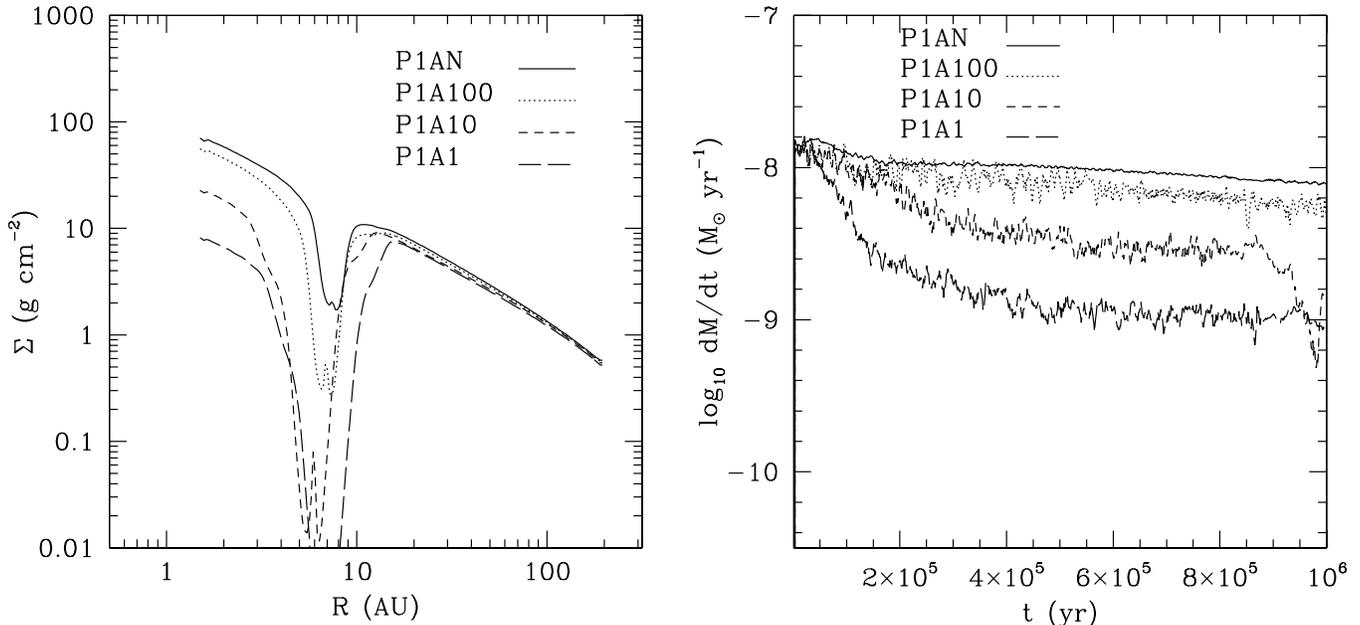[8] Although their $f = 0.1$, the radius within which mass is added to the planet is 0.2 Hill radii.

Figure 1. Left: disk surface densities at 0.5 Myr for viscous disks ($\alpha = 0.01$) with one planet accreting at different rates: no planet accretion (solid curve), accretion on 100 ($f = 100$; dotted curve), 10 ($f = 10$; short-dashed curve), and 1 orbital timescales ($f = 1$; long-dashed curve; see the text for further explanation). Right: the disk accretion rates onto the central star for these four cases. A comparison between the left and right panels demonstrates that the depletion of the inner disk surface density results in a proportional decrease in accretion rate onto the central star.
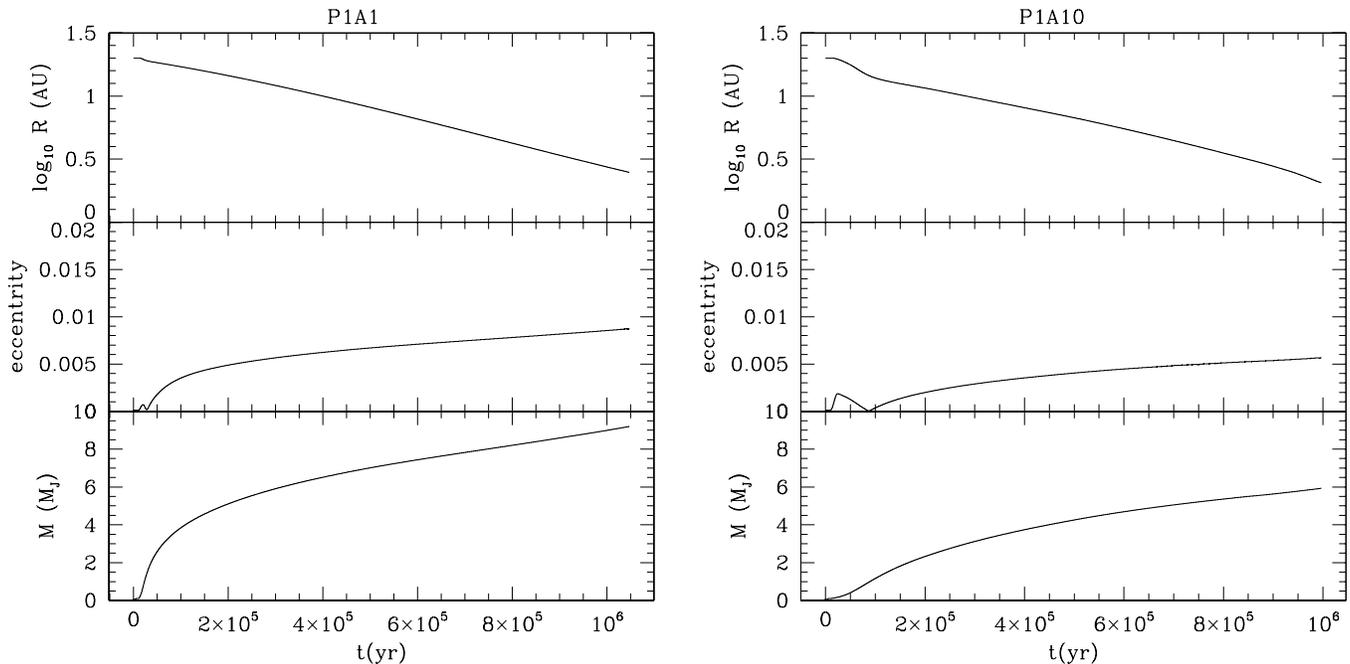
Figure 2. Planet's semimajor axis, eccentricity, and mass as a function of time for the P1A1 case (left) and the P1A10 case (right).

decay or nearly constant behavior, depending upon how fast the planet mass grows (which affects the mass transfer through the gap). With α as large as 0.01, the gap is shallow and the planet is not fully locked to the viscous evolution of outer edge of the gap, as there remains significant mass flow through the gap. The resulting planet migration timescale is $\sim 10^6$ yr (Figure 2) while the viscous timescale at that radius is 1.8×10^5 yr; thus the planet does not migrate very far during the viscous timescale, allowing the inner disk mass accretion rate to approach a steady state. The reason for the migration being so much slower than the viscous evolution rate is that the flow of gas through the gap causes a positive corotation torque to be exerted on the planet (Masset

2002), reducing the rate of inward migration. This timescale estimate also suggests that if α is as large as 0.01, the supply of gas to accrete onto the star in transitional and pre-transitional disks must come from the outer disk to be sustained for ~ 1 Myr.

4.2. Viscous Disks with Two Planets

Figure 3 shows the cases (P2A) with two accreting planets originally placed at 12.5 and 20 AU. The gap opened by the joint action of the two planets is considerably wider than in the single planet case (by roughly a factor of three between the outer and inner edge of the gap).
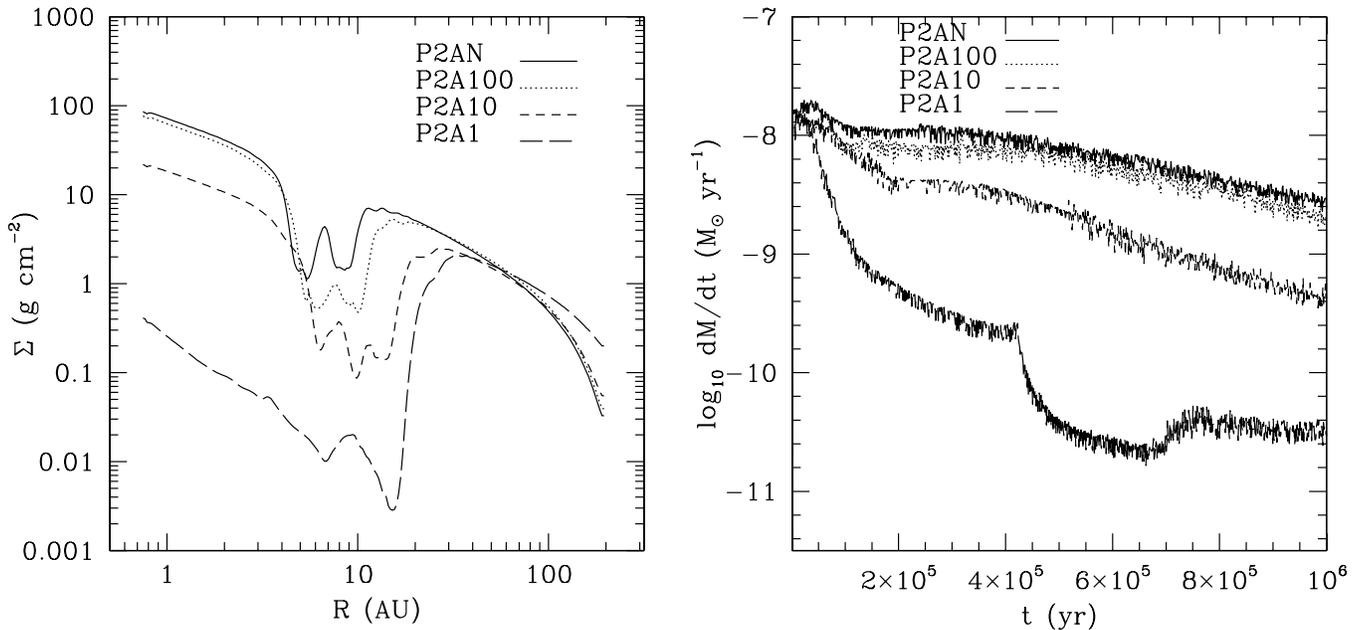
Figure 3. Left: disk surface densities at 0.5 Myr for two planets with no planet accretion (solid curve), $f = 100$ (dotted curve), $f = 10$ (short-dashed curve), and $f = 1$ (long-dashed curve). Right: the disk accretion rates onto the central star for these four cases.

If neither of the planets is accreting (P2AN), the inner disk surface density (solid curve in Figure 3) and the mass accretion rate onto the star are close to the no planet case as expected after a period of initial relaxation. However, if both of the planets are accreting rapidly ($f = 1$; P2A1) the accretion rate onto the central star and the surface density in the disk interior to the gap are both reduced by almost two orders of magnitude (long-dashed curve in Figure 3), as expected since each planet accretes roughly 90% of the viscous flow, leaving only 1% to make it through the gap.

The planets' orbital properties for the P2A1 case are shown in the left panel of Figure 4. The two planets migrate inward at a significantly slower rate than in the one planet case (Kley 2000; compare Figure 2). Due to the common gap formed by two planets, the torque from the outer disk on the inner planet is almost zero. Although the outer planet tries to migrate toward the inner planet, the latter pushes the outer planet outward by locking it into 2:1 resonance. The eccentricity of the planets is also driven up as they move into 2:1 resonance (Figure 4), as seen in other simulations (e.g., Snellgrove et al. 2001; Kley et al. 2005; Pierens & Nelson 2008). The outer planet's mass grows faster than the inner planet because the outer planet is continuously being fed by material from the outer disk.

With median and slow planet accretion rates ($f = 10$ and 100, cases P2A10 and P2A100), the disk accretion rates onto the central star and the inner disk surface densities are reduced by factors similar to that of the equivalent single planet cases. Unlike the P2A1 case, both of these planets almost grow at the same rate (right panel of Figure 4) because there is enough mass flow passing the outer planet to feed the inner planet.

4.3. Viscous Disks with Three and Four Planets

Including more giant planets in the disk produces wider gaps, as expected (see Figures 5 and 7 for the case with three and four planets, respectively). However, the greater the number of planets that are present, the more the accretion flow reaching the inner disk is reduced. Fast planetary accretion ($f = 1$) quickly results in decreasing both the inner disk surface density and

the mass accretion rate by more than two orders of magnitude, while median and slow planet accretion ($f = 10$ and 100) lead to less than one order of magnitude reduction initially. There is a longer-term decay of the mass accretion rate, which is due to the fact that the inclusion of more planets disturbs the disk more, and over long timescales this causes mass to be depleted from the disk as it escapes through the open outer boundary.

The planets' orbital properties are shown in Figures 6 and 8. In most cases, the planets are trapped into 2:1 resonances between each pair of adjacent planets. The middle panel of Figure 8 displays the time evolution of the resonant angle $\phi = 2\lambda_O - \lambda_I - \varpi_I$ associated with the 2:1 resonance, where $\lambda_I(\lambda_O)$ and $\varpi_I(\varpi_O)$ are respectively the mean longitude and longitude of pericenter of the inner (outer) planet of the pair. Whenever the resonant angle librates between the interval $[-\pi, \pi]$ the planets are trapped in a 2:1 resonance. The smaller the amplitude of libration, the deeper resonance locking. As in the two-planet case (Figure 4), the planets' migration slows down due to resonance locking, possibly as a result of the growth of planetary eccentricity which can reduce the migration torques, and also due to the larger inertia associated with a resonant multi-planet system.

There are two cases, however, where planets experience a close encounter and are gravitationally scattered. The first case is P3A1 (left panel in Figure 6), where the eccentricity of the middle planet is driven so high that its orbit overlaps with the inner planet's orbit, leading the inner planet to be scattered out from this system (in a hyperbolic orbit). The second case is P4AN (left panel in Figure 8), where the innermost two planets slip out of 2:1 resonance leading to scattering. In this case, the planets remain bound but switch their positions. It is clear that the disk model with $\alpha = 0.01$ leads to circumstances where three or four planet resonances can be maintained stably over Myr timescales but can also lead to the break up of the resonances. This diversity of behavior appears to have a strong stochastic component, such that the stability of the planet system depends on the detailed history of disk–planet and planet–planet interactions.
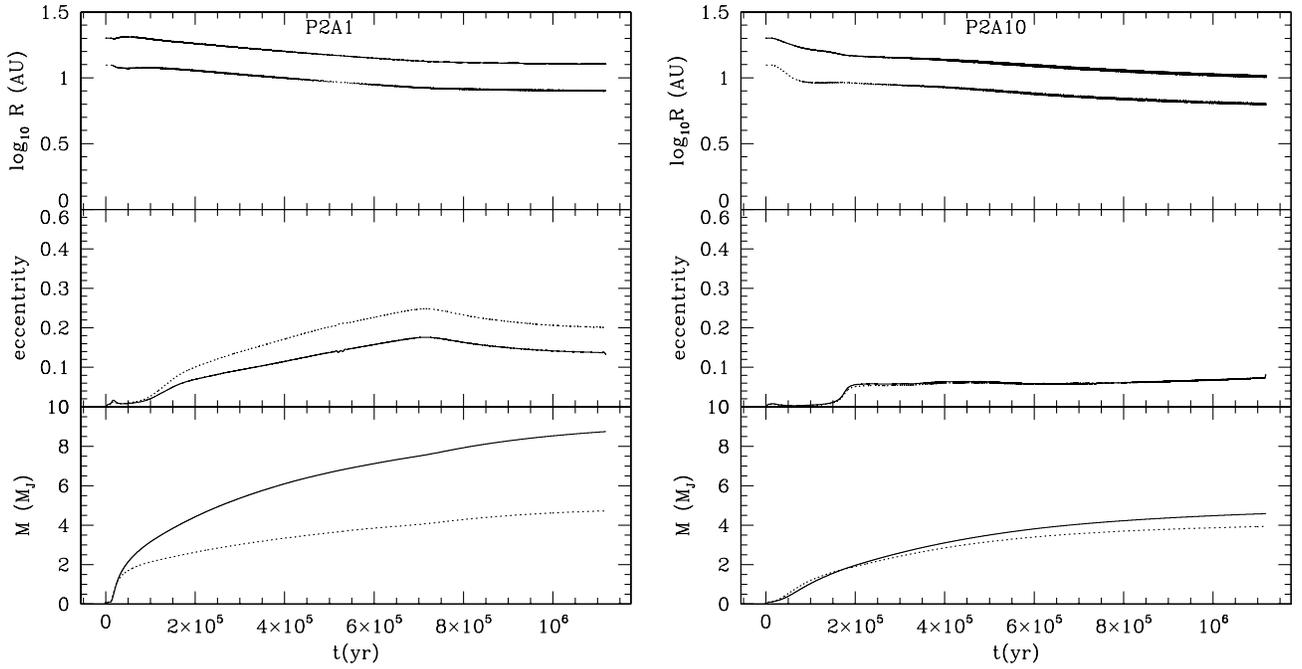
Figure 4. Planets' semimajor axis, eccentricities, and masses as a function of time for the two accreting planets in the P2A1 case (left) and the P2A10 case (right). The solid curves represent the outer planet while the dotted curves represent the inner planet.
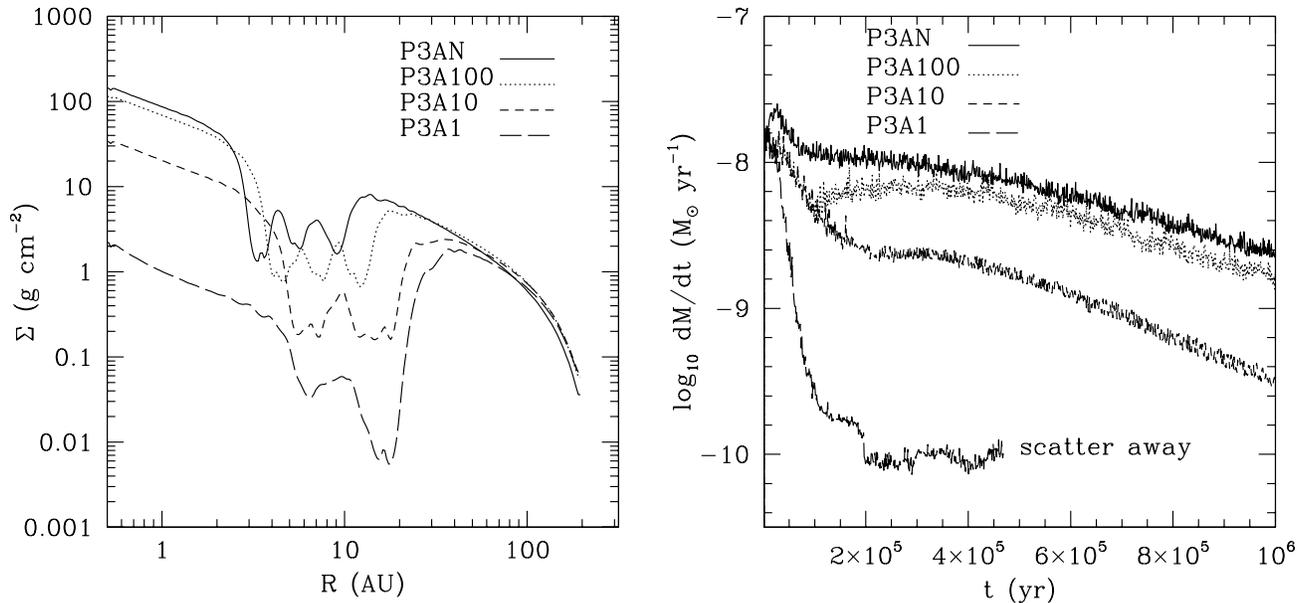

Figure 5. Left: disk surface densities at 0.4 Myr for three planets with no planet accretion (solid curve), $f = 100$ (dotted curve), $f = 10$ (short-dashed curve), and $f = 1$ (long-dashed curve). Right: the corresponding disk accretion rates.

We also performed some limited calculations of three or four planets in disks with a lower viscosity ($\alpha = 0.002$) and a higher disk mass to give the same disk accretion rate. In contrast to the lower mass $\alpha = 0.01$ disks, these models all produced unstable planet systems which resulted in scattering and ejection of at least one planet from the system. This apparently occurs for two reasons. The first is that the low α disks result in deeper gaps, leading to a reduction in the eccentricity damping provided by the disk, thus favoring planetary instability. Second, the significantly larger disk mass probably has a more important dynamical influence on the resonant planetary systems, possibly helping to render the resonant configuration unstable. We will consider the effect of varying the viscosity in more detail in a future paper.

5. DISCUSSION

Returning to the questions posed at the end of Section 1, our findings are as follows.

1. As seen in previous simulations, a single planet opens up a small gap. Multiple planets can open wider common gaps. However, in order to explain the pre-transitional disk gaps spanning almost an order of magnitude in radius without dust depletion (Section 2), we need as many as three to four giant planets, given the tendency of the viscously evolving disk to drive the planets into 2:1 resonances. This is a large number of such planets, given current exoplanet statistics which do not include examples of systems containing more than two planets in resonance. One possibility is
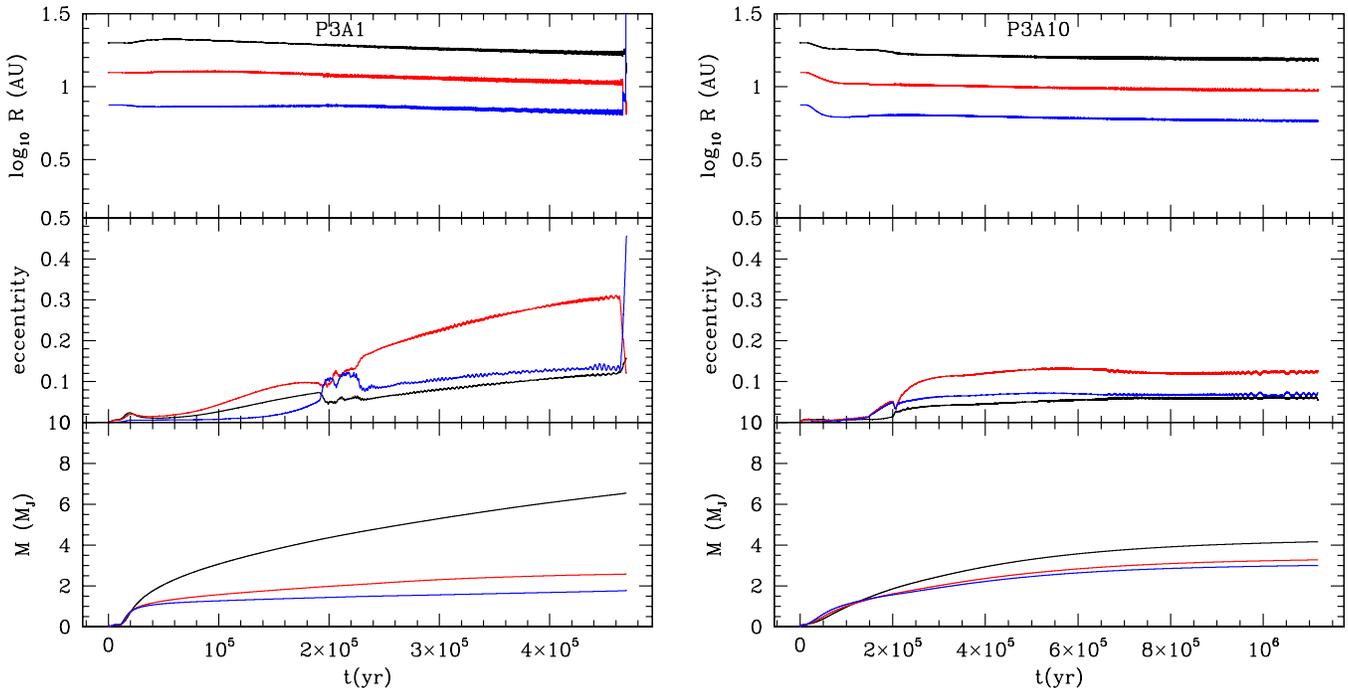
Figure 6. Planets' semimajor axis, eccentricities, and masses as a function of time for three accreting planets in the P3A1 case (left) and the P3A10 case (right). (A color version of this figure is available in the online journal.)

that resonant planet systems which contain more than two planets are able to remain stable over significant time periods (∼1 Myr) in the presence of the gas disk, whose contribution to eccentricity damping helps maintain dynamical stability. Once the gas disk dissipates, however, these resonant planetary systems may become unstable, leading eventually to ejection of some members and the formation of more sparsely populated systems of planets on eccentric orbits, similar to those observed. According to this hypothesis, large systems of planets help explain the presence of the large disk gaps in pre-transitional disks and also explain the population of eccentric giant exoplanets.

In principle, the gaps could be widened for fewer planets if the orbits were eccentric; however, with large $\alpha = 0.01$, we do not see high eccentricities in stable systems.

2. A high accretion rate past the planetary gap can be maintained if accretion onto the planets is sufficiently slow. Planetary accretion rates of $f = 10$ still permit substantial accretion (>10% accretion rate outside the gap) past the planets to the inner disk. However, the reduction in surface density interior to the gap is in proportion to the reduction in mass accretion rate. This differs from the results of Varnière et al. (2006) but is consistent with the results of Crida et al. (2007), and is almost certainly the result of the improved treatment of the inner boundary condition.

3. Carefully comparing our simulations with observations indicates that the pre-transitional/transitional disk systems require substantial reduction in dust opacities within the gaps (and inner disk if present) since the reductions in surface density there are not sufficient to explain the very small amount of dust required to fit the observations. For example, if we adopt the ISM opacity at 10 μm (the assumption used by Espaillat et al. (2010) to estimate optically thin dust masses) of $\kappa \sim 10$ cm^2 g^{-1}, even the gaps with surface densities $\Sigma \gtrsim 0.1$ g cm^{-2} are still

optically thick, which is the case for all but the $f = 1$ simulations. $f = 1$ simulations still have optical depth ∼0.1 and they are the cases with an extreme upper limit on the expected planetary accretion rate, which leads to low accretion rate onto the star (especially with multiple planets). Furthermore, the dust depletion must be larger in the inner disk than in outer regions. This follows from our adoption of a realistic temperature distribution and improved inner boundary condition, which results in a significantly higher surface density at small radii than at large radii; thus the inner disk will not be optically thin unless the outer disk is also optically thin, which disagrees strongly with transitional disk observations.

One alternative is to place planets sufficiently close to the central star that the gap essentially extends either up to the dust destruction radius or near to it; however, in that case it is difficult to extend the gap all the way out to 20–70 AU as observed (Table 1) when using only four planets. In principle it may be possible to accommodate additional planets at smaller orbital radii which truncate the inner disk to a smaller radius. The other alternative is to allow the planets to accrete more mass, depleting the inner disk; but then the mass accretion rate onto the central star is reduced by unacceptably large values.

Protoplanetary disks are probably not fully viscous (e.g., Gammie 1996), but the existence of "dead zones" and/or reduced viscosity regions is unlikely to improve the situation, as they will lead to higher surface densities for a given mass accretion rate, and may reduce the stability of systems of more than two planets in resonance.

5.1. Gap Structure and Dust Depletion

A multi-giant planet model coupled with substantial dust depletion in the gap and inner disk does have an attractive feature. As pointed out in Section 2, there is some evidence—both from SED modeling and from near-infrared interferometry—that the
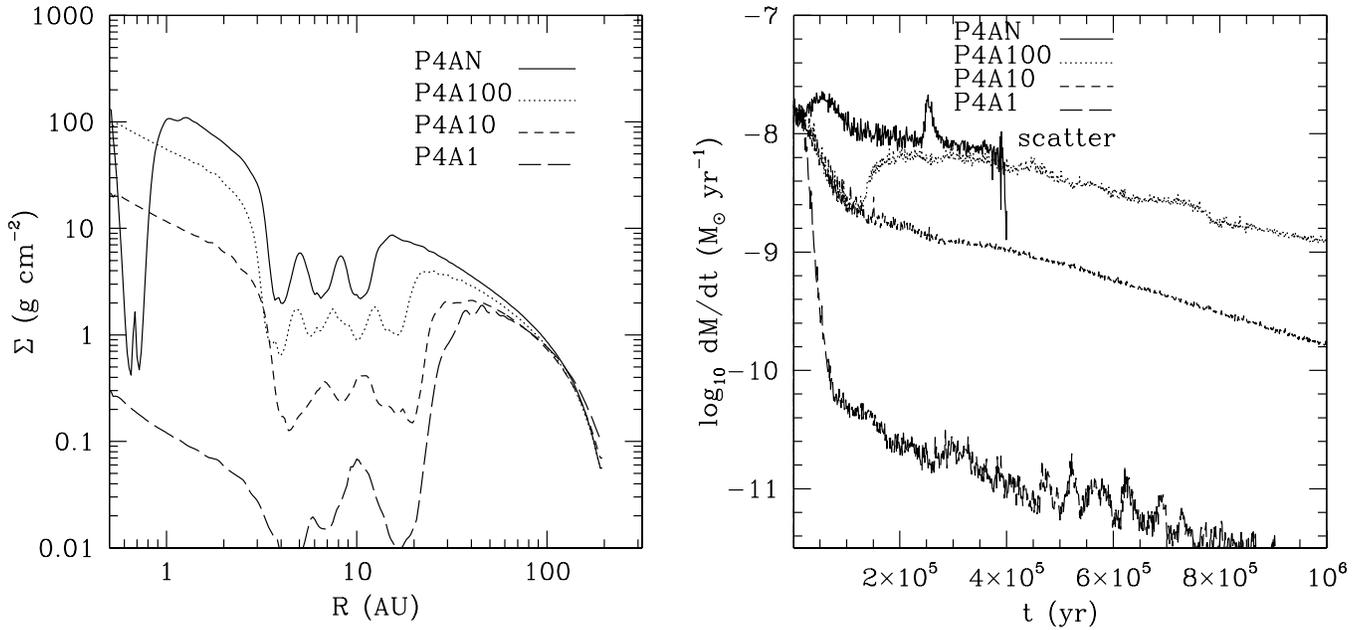
Figure 7. Left: disk surface densities at 0.4 Myr for four planets with no planet accretion (solid curve), $f = 100$ (dotted curve), $f = 10$ (short-dashed curve), and $f = 1$ (long-dashed curve). Right: the corresponding disk accretion rates.
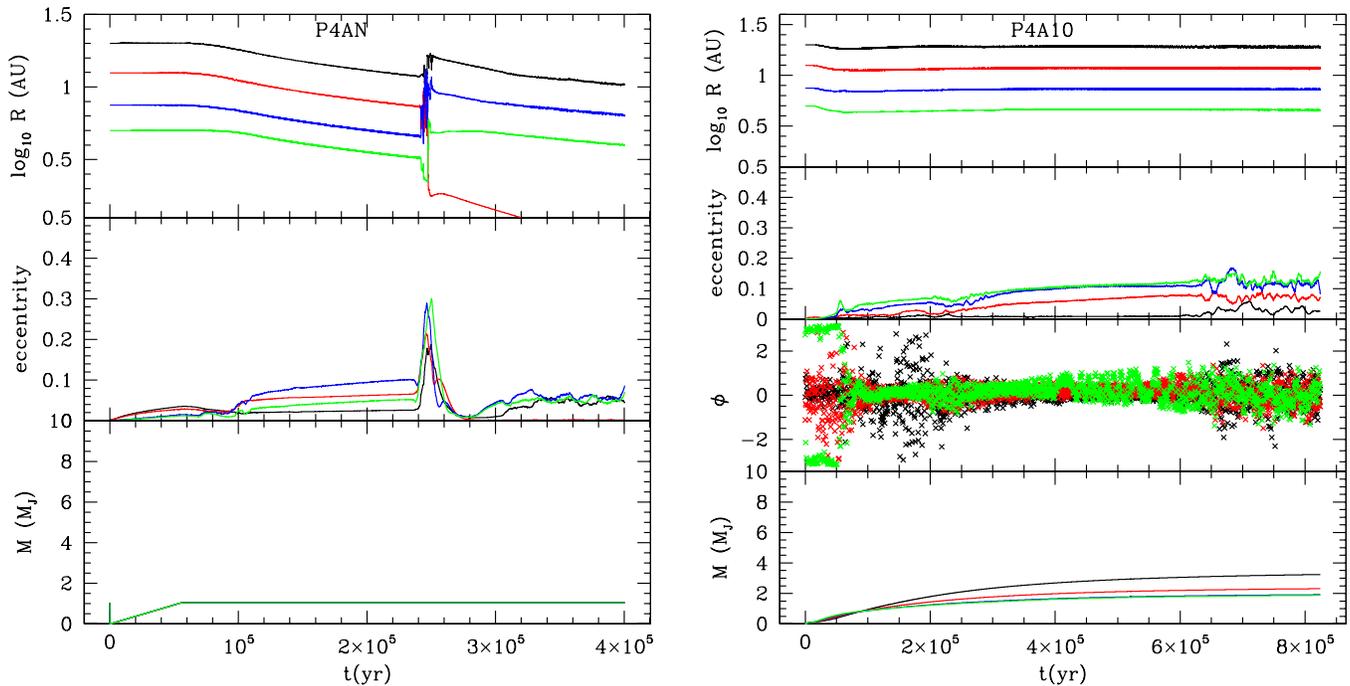

Figure 8. Planets' semimajor axis, eccentricities, resonant angles (2:1), masses with time for four planets in the P4AN case (left) and the P4A10 case (right). In the ϕ panel of the right figure, black, red, and green curves represent the resonant angle between the pairs of 4/3, 3/2, 2/1 planets (4 is the outermost one).
(A color version of this figure is available in the online journal.)

pre-transitional and transitional disks exhibit structure within the optically thin disk gap or hole, such that the innermost gap region is much less cleared of small dust than the outer gap region. Schematically, we might identify the highly cleared region with the true planet-driven gap, and the inner, optically thin dust region with accreting gas that has been strongly depleted in dust but not so depleted in gas surface density. The idea is illustrated in Figure 9, which compares the inferred structure of one of the pre-transitional disk systems with the azimuthally averaged dust surface density for the P4A10 case.

In Figure 9, the disk optical depth at 10 μm can be estimated by multiplying the dust surface density (dust refers to small dust particles which contribute to 10 μm opacity) by 1000 cm^2 g^{-1} (which is estimated using the ISM opacity: a factor of 100 comes from the gas-to-dust mass ratio and 10 cm^2 g^{-1} is the ISM opacity at 10 μm). Thus, disk regions with dust surface density $> 10^{-3}$ g cm^{-2} are optically thick. The dotted curve represents the dust surface density resulting from the model P4A10 assuming there is no dust depletion, which is obtained by dividing the gas surface density from the P4A10 simulation
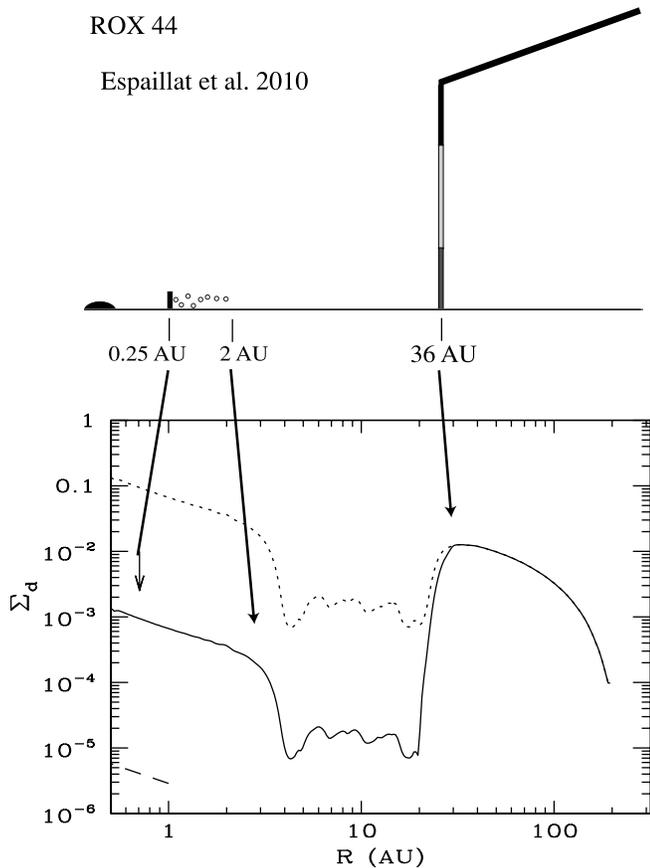
Figure 9. Pre-transitional disk structure taken from Espaillat et al. (2010) compared with the azimuthal-averaged dust surface density of the P4A10 case. The dotted curve represents the case with no dust depletion and the solid curve represents the case with the dust at the inner disk depleted by a factor of 100. The solid curve can explain the pre-transitional disk structure as indicated by the arrows. The dashed curve is the dust surface density from the transitional disk GM Aur estimated by Equation (9), which requires the dust to deplete by a factor of 10^5 by comparison with the dotted curve.

by the nominal gas-to-dust mass ratio ~ 100. In this case, even the gap is optically thick. The solid curve represents the case where we notionally deplete the dust content inside the gap by a factor of 100. This can explain the pre-transitional disks whose inner region within ~ 1 AU changes from being optically thick to optically thin, with the region beyond being almost dust free. This comparison with pre-transitional disks set a lower limit on the dust depletion factor, while the transitional disks can set a higher limit. If we assume all the dust inside the transitional disk gap has been detected (which is reasonable since transitional disks are optically thin), we can estimate the dust surface density by solving

$$\int_0^{R_{\text{out,thin}}} \Sigma_d(R) 2\pi R\, dR = M_d, \qquad (9)$$

where $R_{\text{out,thin}}$ and M_d are given in Table 1, and is assumed to be $\Sigma_d(\text{AU})(R/\text{AU})^{-1}$. The derived Σ_d for GM Aur (<1 AU) using Table 1 is shown as the dashed curve in Figure 9. By comparing with the dotted curve, we find the dust needs to deplete by a factor of $\sim 10^5$. Thus we estimate the dust-to-gas mass ratio in the inner disk is between 10^{-5} and 10^{-2} of the ISM value (0.01) for our model to be consistent with pre-transitional/transitional disks.

More broadly, a gap-opening perturbing body or bodies still remains a plausible explanation of the pre-transitional/

transitional disks. This type of model naturally predicts a sharp transition in surface density at the outer gap edge, which is needed to explain the strong mid- and far-infrared emission of these systems. While radially dependent dust depletion might also mimic this effect, most T Tauri disks do not show this behavior. There are a significant number of T Tauri systems in which the disk is optically thick at a wide range of radii, but which are much more geometrically flat based on their SEDs (e.g., the "group E" systems shown in Figure 7 of Furlan et al. 2006). These objects suggest that dust growth and settling can occur roughly simultaneously over a wide range of radii, without resulting in the abrupt change between optically thin and optically thick regions that occurs in the pre-transitional/ transitional disks. In addition, the large outer disk gap radii (as much as 20–70 AU) pose a challenge for pure coagulation models at an age of ~ 1–2 Myr (Tanaka et al. 2005; Dullemond & Dominik 2005).

The requirement of significant dust depletion is not completely surprising, given the evidence for small dust depletion in many T Tauri disks without obvious gaps or holes (e.g., D'Alessio et al. 2001; Furlan et al. 2006). In addition, formation of giant planets via core accretion clearly requires dust growth. Indeed, an outstanding theoretical problem has been to avoid clearing inner disks by ages of 1 Myr or less (e.g., Dullemond & Dominik 2005; Tanaka et al. 2005), resulting in suggestions that small dust must be replenished to some extent by fragmentation as a result of collisions of larger particles.

A hypothesis which explains many features of pre-transitional/transitional disks using both giant planets and dust depletion can be outlined as follows. Dust coagulation and growth in the disk interior to ~ 20 AU ensues, leading to the formation of planetesimals, and eventually to the formation of a system of numerous giant planets. This system of giant planets forms a large common gap which covers radii from <1 AU out to ~ 50 AU. Remnant planetesimals within the gap region, whose collisions can act as a secondary source of dust, are dynamically cleared out—preventing in situ secondary dust formation. After a viscous timescale corresponding to the size scale of the planetary system, the gas present in the planet-induced gap and the inner disk within 1 AU has originated largely from that part of the disk which lies out beyond the planetary system. This gas may be substantially depleted of small dust because of significant grain growth at large radii, combined with filtration of dust at the outer edge of the gap (Paardekooper & Mellema 2006; Rice et al. 2006). Furthermore, small dust particles may manage to pass through the gap, but they can quickly coagulate to big dust particles (Dullemond & Dominik 2005). In this scenario, gas which accretes through the system at late times is strongly depleted of dust, can sustain a significant accretion rate onto the central star, and can provide a dust-rich wall at the outer edge of the gap required by SED modeling. We will explore this hypothesis in a forthcoming paper in which we include the effects of dust filtration.

5.2. Numerical Limitations

Our simulations are highly simplified, and this needs to be borne in mind when interpreting our results. The resolution we adopt is insufficient to resolve the gas flow within the planet Hill sphere, and so we are forced to adopt a simplified approach to simulating gas accretion onto the planet, instead of simulating the accretion process directly. As such the detailed evolution of the gas flow in and around the planet Hill sphere may not be modeled with a high degree of fidelity in our

simulations. The simulations are 2D, which may not be a good approximation early on when the planet masses are low, but improves as the planet masses become large and gap formation occurs. We have neglected a detailed treatment of the gas thermodynamics, adopting instead a locally isothermal equation of state. A proper treatment would allow the local disk temperature to be determined by a balance between viscous and stellar heating, and radiative cooling, and this might affect details of the gap structure due to the changing optical depth of the gas and its thermal evolution there (although viscous heating is generally much smaller than stellar heating). Ayliffe & Bate (2010) suggest radiation due to circumplanetary disk accretion tends to suppress the spiral shocks and leads to a shallower gap (their Figure 18), which only increases the need for dust depletion within the gaps. Finally, we do not explicitly simulate the MHD turbulence that is believed to provide the effective viscous stresses in protoplanetary disks (Balbus & Hawley 1991). But it appears from previous simulations that adopting the usual α prescription gives results in broad agreement with MHD simulations when considering gap formation and giant planet migration (Nelson & Papaloizou 2003; Winters et al. 2003; Papaloizou et al. 2004). As such, we do not expect that the qualitative nature of our results has been compromised by the neglect of the above physical processes.

6. SUMMARY

In this paper, we present 2D hydrodynamic simulations to explore the possibility that the properties of pre-transitional/transitional disks are due to gap opening by planets in viscous disks. With an improved inner boundary condition, we found that the surface density of the disk interior to the planet-formed gap is depleted by the same factor as the mass accretion rate through the gap and into the inner disk is reduced. Thus, the substantial accretion rates of pre-transitional/transitional disks require substantial gas surface densities inside of planet-driven gaps. We also found that even multiple planets have difficulty in making large disk gaps and holes which are deep enough to explain the observations. Thus small grain depletion seems to be an essential part of the explanation of the structure of pre-transitional/transitional disks, and this may be explained by the dust growth or the accretion of grain-depleted gas from large disk radii at late times and dust filtration. In addition, multiple planets might account for the inferred structure within the gaps of pre-transitional/transitional disks, in which the inner gaps are much less cleared of small dust than outer gap regions.

REFERENCES

Akeson, R. L., et al. 2005, ApJ, 635, 1173
Alexander, R. D., & Armitage, P. J. 2007, MNRAS, 375, 500
Alexander, R. D., & Armitage, P. J. 2009, ApJ, 704, 989
Andrews, S. M., & Williams, J. P. 2005, ApJ, 631, 1134
Andrews, S. M., Wilner, D. J., Hughes, A. M., Qi, C., & Dullemond, C. P. 2009, ApJ, 700, 1502
Ayliffe, B. A., & Bate, M. R. 2009, MNRAS, 397, 657
Ayliffe, B. A., & Bate, M. R. 2010, MNRAS, 408, 876
Balbus, S. A., & Hawley, J. F. 1991, ApJ, 376, 214
Brown, J. M., Blake, G. A., Qi, C., Dullemond, C. P., Wilner, D. J., & Williams, J. P. 2009, ApJ, 704, 496
Brown, J. M., et al. 2007, ApJ, 664, L107
Calvet, N., D'Alessio, P., Hartmann, L., Wilner, D., Walsh, A., & Sitko, M. 2002, ApJ, 568, 1008
Calvet, N., et al. 2005, ApJ, 630, L185
Clarke, C. J., Gendrin, A., & Sotomayor, M. 2001, MNRAS, 328, 485
Crida, A., & Morbidelli, A. 2007, MNRAS, 377, 1324
Crida, A., Morbidelli, A., & Masset, F. 2007, A&A, 461, 1173
D'Alessio, P., Calvet, N., & Hartmann, L. 2001, ApJ, 553, 321
D'Alessio, P., et al. 2005, ApJ, 621, 461
de Val-Borro, M., et al. 2006, MNRAS, 370, 529
Dullemond, C. P., & Dominik, C. 2005, A&A, 434, 971
Espaillat, C., Calvet, N., D'Alessio, P., Hernández, J., Qi, C., Hartmann, L., Furlan, E., & Watson, D. M. 2007, ApJ, 670, L135
Espaillat, C., Calvet, N., Luhman, K. L., Muzerolle, J., & D'Alessio, P. 2008, ApJ, 682, L125
Espaillat, C., et al. 2010, ApJ, 717, 441
Furlan, E., et al. 2006, ApJS, 165, 568
Gammie, C. F. 1996, ApJ, 457, 355
Gorti, U., & Hollenbach, D. 2009, ApJ, 690, 1539
Gullbring, E., Hartmann, L., Briceno, C., & Calvet, N. 1998, ApJ, 492, 323
Hartmann, L., Calvet, N., Gullbring, E., & D'Alessio, P. 1998, ApJ, 495, 385
Hughes, A. M., et al. 2009, ApJ, 698, 131
Kley, W. 2000, MNRAS, 313, L47
Kley, W., Lee, M. H., Murray, N., & Peale, S. J. 2005, A&A, 437, 727
Lin, D. N. C., & Papaloizou, J. 1986, ApJ, 307, 395
Lin, D. N. C., & Papaloizou, J. C. B. 1993, Protostars and Planets III, 749
Lubow, S. H., & D'Angelo, G. 2006, ApJ, 641, 526
Marsh, K. A., & Mahoney, M. J. 1992, ApJ, 395, L115
Masset, F. 2000, A&AS, 141, 165
Masset, F. S. 2002, A&A, 387, 605
Masset, F. S., & Papaloizou, J. C. B. 2003, ApJ, 588, 494
Movshovitz, N., Bodenheimer, P., Podolak, M., & Lissauer, J. J. 2010, Icarus, 209, 616
Najita, J. R., Carr, J. S., Strom, S. E., Watson, D. M., Pascucci, I., Hollenbach, D., Gorti, U., & Keller, L. 2010, ApJ, 712, 274
Najita, J. R., Strom, S. E., & Muzerolle, J. 2007, MNRAS, 378, 369
Natta, A., Prusti, T., Neri, R., Wooden, D., Grinin, V. P., & Mannings, V. 2001, A&A, 371, 186
Nelson, R. P., & Papaloizou, J. C. B. 2003, MNRAS, 339, 993
Nelson, R. P., Papaloizou, J. C. B., Masset, F., & Kley, W. 2000, MNRAS, 318, 18
Owen, J. E., Ercolano, B., Clarke, C. J., & Alexander, R. D. 2010, MNRAS, 401, 1415
Paardekooper, S.-J., & Mellema, G. 2006, A&A, 453, 1129
Papaloizou, J. C. B., & Nelson, R. P. 2005, A&A, 433, 247
Papaloizou, J. C. B., Nelson, R. P., & Snellgrove, M. D. 2004, MNRAS, 350, 829
Pierens, A., & Nelson, R. P. 2008, A&A, 482, 333
Piétu, V., Dutrey, A., Guilloteau, S., Chapillon, E., & Pety, J. 2006, A&A, 460, L43
Pollack, J. B., Hubickyj, O., Bodenheimer, P., Lissauer, J. J., Podolak, M., & Greenzweig, Y. 1996, Icarus, 124, 62
Pott, J.-U., Perrin, M. D., Furlan, E., Ghez, A. M., Herbst, T. M., & Metchev, S. 2010, ApJ, 710, 265
Rice, W. K. M., Armitage, P. J., Wood, K., & Lodato, G. 2006, MNRAS, 373, 1619
Rice, W. K. M., Wood, K., Armitage, P. J., Whitney, B. A., & Bjorkman, J. E. 2003, MNRAS, 342, 79
Schneider, G., Wood, K., Silverstone, M. D., Hines, D. C., Koerner, D. W., Whitney, B. A., Bjorkman, J. E., & Lowrance, P. J. 2003, AJ, 125, 1467
Snellgrove, M. D., Papaloizou, J. C. B., & Nelson, R. P. 2001, A&A, 374, 1092
Stone, J. M., & Norman, M. L. 1992, ApJS, 80, 753
Tanaka, H., Himeno, Y., & Ida, S. 2005, ApJ, 625, 414
Varnière, P., Blackman, E. G., Frank, A., & Quillen, A. C. 2006, ApJ, 640, 1110
Winters, W. F., Balbus, S. A., & Hawley, J. F. 2003, ApJ, 589, 543